Intermittency in ^{197}Au fragmentation

M. L. Cherry,[2] A. Dąbrowska,[1] P. Deines-Jones,[2] R. Hołyński,[1] W. V. Jones,[2] A. Olszewski,[1] E. A. Pozharova,[4] K. Sengupta,[2] T. Yu. Skorodko,[4] M. Szarska,[1] C. J. Waddington,[3] J. P. Wefel,[2] B. Wilczyńska,[1] W. Wolter,[1] and B. Wosiek[1]

(The KLMM Collaboration)

[1]*Institute of Nuclear Physics, Kawiory 26A, 30-055 Kraków, Poland*

[2]*Deptartment of Physics and Astronomy, Louisiana State University, Baton Rouge, Louisiana 70803*

[3]*School of Physics and Astronomy, University of Minnesota, Minneapolis, Minneapolis 55455*

[4]*Institute of Theoretical and Experimental Physics, B. Cheremushkinskaya 25, 117-259 Moscow, Russia*

(Received 5 September 1995)

The concept of factorial moments was applied to an analysis of the dynamical fluctuations in the charge distributions of the fragments emitted from gold nuclei with energies 10.6 and <1.0 GeV/nucleon interacting with emulsion nuclei. Clear evidence for intermittent fluctuations has been found in an analysis using all the particles released from the gold projectile, with a stronger effect observed below 1 GeV/nucleon than at 10.6 GeV/nucleon. For the full data sets, however, the intermittency effect was found to be very sensitive to the singly charged particles, and neglecting these particles strongly reduces the intermittency signal. When the analysis is restricted to the multiply charged fragments, an intermittency effect is revealed only for multifragmentation events, although one that is enhanced as compared to the analysis of all, singly and multiply charged, particles. The properties of the anomalous fractal dimensions suggest a sequential decay mechanism, rather than the existence of possible critical behavior in the process of nuclear fragmentation. The likely influence of the charge conservation effects and the finite size of decaying systems on the observed intermittency signals was pointed out.

PACS number(s): 25.75.Gz, 29.40.Rg

I. INTRODUCTION

The concept of intermittency was originally developed in the field of fluid dynamics to study the fluctuations that occur in turbulent flow [1,2]. Its presence in the velocity and temperature distributions is established by the existence of large nonstatistical fluctuations which exhibit scale invariance. Intermittency in physical systems is studied by examining the scaling properties of the moments of the distributions of relevant variables over a range of scales [3]. Białas and Peschanski [4] first introduced the concept of intermittency to the study of dynamical fluctuations in the density distributions of particles produced in high energy collisions. In order to identify any intermittent behavior in the physical processes occurring during these collisions, they proposed an analysis of the scaling properties of the factorial moments, F_q, as the resolution in the density distribution was varied. By using the method of factorial moments, which results in a filtering out of the statistical fluctuations, it was possible to analyze data on particle production. This soon led to the discovery of a characteristic power law dependence of the factorial moments of an order q on the resolution scale, δ: $F_q \propto (1/\delta)^{\varphi_q}$. This feature of the moments, identified as an example of intermittency, was observed in a variety of high energy reactions [5–7] and can be considered to be a general property of the particle production process. The specific properties of the intermittency indices, φ_q, can be associated either with a random cascading process [4,8–11] or with a second-order phase transition [9,12–14] depending on the values obtained. Thus an analysis of the factorial moments may provide important information on the dynamical properties of the system. A similar analysis can be applied to other processes, such as nuclear fragmentation, in order to attain a better understanding of the physics involved.

Płoszajczak and Tucholski [15] were the first to suggest searching for intermittency patterns in the mass and charge distributions of the fragments produced during the collisions of energetic nuclei. They studied the breakup of ^{197}Au nuclei with energies below 1 GeV/nucleon, and showed that the factorial moments of the charge distribution of the fragments increased like a power law with increasing charge resolution, thus exhibiting the property of intermittency. A similar analysis, confirming the existence of intermittency in nuclear fragmentation, was later applied to the breakup of ^{238}U and ^{131}Xe nuclei with $E \leqslant 1$ GeV/nucleon [16]. However, as yet there is no clear understanding of the underlying dynamical mechanism that leads to intermittency in nuclear fragmentation. No clear evidence of critical behavior was observed in these studies. It was shown [15] that a percolation model [17,18] could lead to fluctuations in the fragment size distributions similar to those observed in the data. In addition, there were some indications that the fragmentation mechanism is a sequential decay process rather than a prompt breakup or falling apart of the nucleus. On the other hand, specific sequential decay models [19] were unable to reproduce the observed intermittency properties of the fragment distributions.

In this paper we have used 10.6 GeV/nucleon ^{197}Au projectile nuclei, with a much higher incident energy than was available previously for such heavy nuclei to make a detailed study of the fluctuations in the charge distributions of the fragments emitted from interactions with the emulsion target

nuclei. This analysis of the factorial moments is compared with a similar analysis of the interactions of low energy ($\leqslant$1 GeV/nucleon) gold nuclei [20]. In order to compare this analysis with previous studies we have considered the case where the singly charged particles have been included. These singly charged particles numerically dominate the analysis, but experimentally a determination of which ones are spectators, and part of the fragmentation process, and which are participants, is not well defined. For this reason we have made two additional analyses, with one representing an attempt to distinguish between the spectators and participants in the individual interactions, and the other restricted only to multiply charged fragments.

The paper is organized as follows: In Sec. II we give a brief summary of the experimental details, as well as some of the general characteristics of the fragmentation of ^{197}Au at 10.6 GeV/nucleon. More details can be found elsewhere [21–24]. The revisions introduced in the study of the low energy gold interactions are also discussed in this section. In Sec. III the method of analysis is briefly reviewed. Section IV contains the results of the analysis of all particles and the comparison with the low energy data. Also the results of the analysis attempting to include only spectator singly charged particles are presented in this section. Section V discusses the analysis restricted to multiply charged fragments. The summary and conclusions are discussed in Sec. VI.

II. FRAGMENTATION

Stacks of BR-2 nuclear emulsion were exposed to gold nuclei accelerated to an energy of 10.6 GeV/nucleon at the Brookhaven AGS (Exp. BNL 868). A minimum bias sample of interactions was found by microscope scanning along the tracks of incident gold nuclei. In every interaction all the tracks produced by charged particles were analyzed. The high energy multiply charged fragments of the gold nuclei were readily separated from the low energy fragments emitted from the target nuclei. The fast singly and doubly charged particles were identified by their grain densities, while the charges of the heavier fragments were measured by delta ray counts with an accuracy better than 5% over the entire charge range. The present analysis is based on 1083 fully analyzed interactions. Events in which the gold projectile apparently survives and no secondary particles are produced were assumed to be noncharge changing interactions, and were excluded from this sample.

For comparison, the interactions of low energy gold nuclei in emulsion were also analyzed. This low energy sample consists of interactions produced by gold nuclei which entered the emulsions with $E \simeq 1.0$ GeV/nucleon and, which, if they did not interact, were brought to rest by energy loss [20]. For this analysis we have selected only the 360 charge changing interactions for which the energy of the gold projectiles was greater than 0.1 GeV/nucleon.[1]

The initial stage of a nucleus-nucleus collision involves the strong interactions between the colliding nuclei, which leads to the creation of new particles, predominately pions. At this 10.6 GeV/nucleon incident energy, the average number of charged created particles was 50.5 ± 2.0, with individual multiplicities that ranged from 0 to > 300. After the initial ''fast'' collision stage, a much slower process of deexcitation of the projectile and target nuclei occurs, accompanied by the emission of nuclear fragments. It is this latter stage of the interaction, and, in particular, the breakup of the gold projectile, that is of interest here. The number of fragments emitted from the projectile, $N_{\rm fr}$, varies widely from event to event. Similarly the charges (Z) of these fragments cover the entire charge range from 1 to 79. In fact we know that fragments with charge $Z=80$ can be produced by charge pickup [25], but we are unable to identify these relatively rare events in this experiment. The multiply charged fragments are readily detected. The number of α particles ($Z=2$) and heavier fragments ($Z \geqslant 3$) in each event was denoted by N_α and N_F, respectively. N_α was typically much greater than N_F. Singly charged fragments, mostly protons with a small admixture of deuterons and tritons, must also be emitted from the excited gold nuclei, but their numbers cannot be determined reliably in this experiment, since they cannot be separated from the produced and interacting singly charged particles. For each interaction we can use charge conservation to evaluate the total number of singly charged particles that were released, N_p. Then $N_p = Z_{\rm Au} - \Sigma_{i=1}^{N} Z_i$, where the summation runs over all multiply charged fragments. These released singly charged particles include both singly charged projectile fragments (spectators, $N_{\rm spect}$) and interacting protons (participants, $N_{\rm part}$); $N_p = N_{\rm spect} + N_{\rm part}$. Experimentally, it is not possible to make a clean separation between the spectators emitted during the fragmentation process and the participants involved in the fast collision stage of the interaction. However, it is possible to use the measured emission angles of the singly charged particles to make an estimate of the number of spectators in each event, and this approach has been used in some of the later analyses to be discussed.

TABLE I. Characteristics of gold fragmentation for 10.6 GeV/nucleon and 0.1–1 GeV/nucleon full data sets.

Sample	^{197}Au (10.6 GeV/nucleon)	^{197}Au (0.1–1 GeV/nucleon)
$N_{\rm events}$	1083	360
$\langle N_p \rangle$	29.74 ± 0.71	16.01 ± 0.89
$\langle N_\alpha \rangle$	4.36 ± 0.09	5.22 ± 0.20
$\langle N_F \rangle$	1.91 ± 0.04	2.30 ± 0.08
$N_p^{\rm max}$	79	69
$N_\alpha^{\rm max}$	15	15
$N_F^{\rm max}$	8	7
$\langle Z^{\rm max} \rangle$	37.99 ± 0.84	44.47 ± 1.36

The average and maximum numbers of the various types of fragment have been listed in Table I. Also listed there is the average charge of the heaviest fragment, $\langle Z^{\rm max} \rangle$. For comparison similar quantities for the sample of low energy gold nuclei have been included in this table. The values listed in Table I show that overall the high energy gold nuclei are more severely broken up than are those of low energy,

[1]The analysis of the low energy gold interactions by Płoszajczak and Tucholski [15] was based on a slightly larger sample without the exclusion of the lowest energy interactions and noncharge changing events.

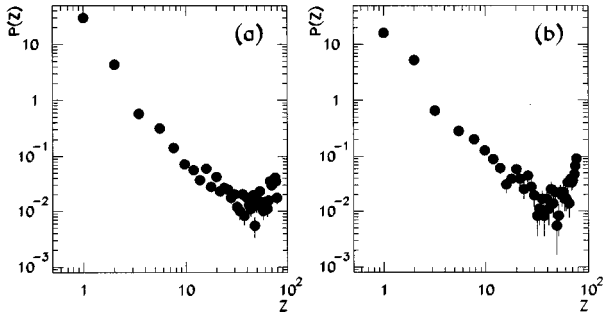

FIG. 1. Yields of charges for fragments from ^{197}Au projectiles measured in full data sets at 10.6 GeV/nucleon (a) and at 0.1–1 GeV/nucleon (b). For $Z \geqslant 3$, two neighbor charges are binned together with the yield plotted at their mean charge.

producing a smaller heaviest fragment and releasing more singly charged particles.

The yields per event of the fragments are shown in Figs. 1(a) and 1(b) for the high and low energy gold interactions. Both data sets show the familiar U-shaped distributions, with the yields rising on both sides from a broad minimum at $Z \approx 0.5 Z_{\mathrm{Au}}$. If we are dealing with a liquid-vapor phase transition at a critical temperature [26,27], or a percolation model [15,17,18], we would expect to observe a power law behavior of the fragments yields, $P(Z) \propto Z^{-\tau}$, with an exponent close to 2.3. Clearly this cannot apply to the entire charge range, since it is well established that the yields of the heaviest fragments increase with increasing charge (see Fig. 1 and also [28]). It is worth noting that the rise in the yields of fragments with Z above 30–40 is due mainly to events in which only a single heavy fragment ($Z \geqslant 3$) is emitted.

It is possible to select subsamples of events for which the charge distribution can be reasonably well described by a single power function. For example, Figs. 2(a) and 2(b) show the charge distributions for events in which 2 or more fragments with $Z \geqslant 3$ are emitted. The fitted inverse power laws in the range $Z \geqslant 3$ gave the values of τ of 1.75 ± 0.04 and 1.56 ± 0.05 at high and low energies, respectively. These fits had reduced χ^2 values of 2.3 and 0.9 in the two cases. The lighter fragments, specifically the helium nuclei, do not fit this representation, there being many more than would be predicted from an extrapolation of these power laws. Inclusion in the fits of the $Z=2$ fragments, even for these selected subsamples of interactions, greatly degrades the quality of the fits, resulting in corresponding χ^2 values of 7.6 and 7.9 for the two energies. The values obtained for τ are smaller than expected from the models. Fragment yields are discussed in more detail elsewhere [29].

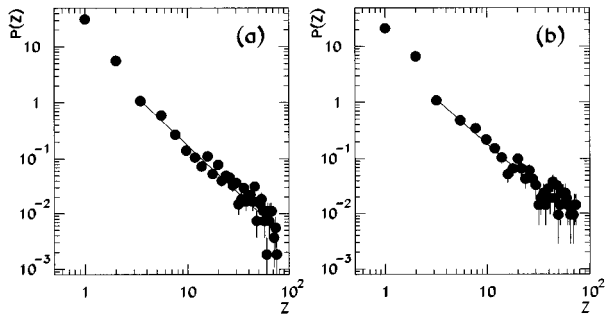

FIG. 2. Yields of charges for fragments from ^{197}Au projectiles measured in a selected subsample of events with $N_F \geqslant 2$ at 10.6 GeV/nucleon (a) and at 0.1–1 GeV/nucleon (b). Lines show the inverse power fits in the range $Z \geqslant 3$.

III. METHOD OF NORMALIZED FACTORIAL MOMENTS

To study intermittency in multiparticle production, Białas and Peschanski [4] suggested analyzing scaled factorial moments of the particle density distributions in decreasing phase space bins, down to the limit of the experimental resolution. The proposed definition of the factorial moments can be extended in a straightforward way to an analysis of the charge distribution of fragments arising from nuclear fragmentation process. For each event the factorial moment, F, of rank q is defined as

$$F_q(\delta Z) = \frac{1}{M} \sum_{m=1}^{M} n_m (n_m - 1) \cdots (n_m - q + 1) / (\bar{N}/M)^q, \tag{1}$$

where M is the number of charge bins into which the whole charge range $\Delta Z = Z_{\max} - Z_{\min}$ has been divided, n_m is the number of fragments emitted in the mth charge bin, $m = 1, \ldots, M$ and $\bar{N}$ is the mean fragment multiplicity measured in the full ΔZ interval. After averaging over all events in the sample, the mean factorial moments are

$$\overline{F_q(\delta Z)} = \frac{\overline{\langle n(n-1)\ldots(n-q+1)\rangle}}{\langle \bar{n} \rangle^q}, \tag{2}$$

where brackets denote averaging over $M = \Delta Z / \delta Z$ bins and bars denote averaging over all events in the sample where there are two or more fragments in the ΔZ interval. Additional correction factors have been proposed [30] to allow for nonuniform distributions of the analyzed variable, leading to a modified definition of the mean factorial moments of the form

$$\overline{F_q^{\mathrm{corr}}(\delta Z)} = \frac{\overline{\langle n(n-1)\cdots(n-q+1)\rangle}}{\langle \bar{n}^q \rangle}. \tag{3}$$

This definition guarantees that in the case of statistical fluctuations, the corrected moments equal unity independently of the bin size, δZ. In what follows, we will only use corrected factorial moments calculated according to Eq. (3) (superscript corr will be omitted for simplicity).

The physical process under study is said to exhibit an intermittent behavior if the factorial moments increase like a power law with decreasing bin size:

$$\overline{F_q(\delta Z)} = \overline{F_q(\Delta Z)} \left(\frac{\Delta Z}{\delta Z} \right)^{\varphi_q}, \tag{4}$$

where $\varphi_q > 0$ in the limit of $\delta Z \to 0$. The magnitude of the exponents, φ_q, called intermittency indices, characterizes the strength of the intermittency signal.

Intermittency occurs in systems which possess the property of self-similarity [Eq. (4)] over a broad range of resolu-

tions. This is a typical feature of fractal objects which also satisfy certain scaling laws. The connection between factorial moments and rules of multifractal geometry reduces to the direct relation between intermittency indices and the anomalous fractal dimensions, d_q of the analyzed distributions [31–33]:

$$d_q = \frac{\varphi_q}{q-1}. \tag{5}$$

It was suggested [9–14] that measurements of anomalous dimensions in the rapidity spectra may reveal an underlying mechanism in particle production processes. Particularly, it was argued [9,13] that an observation of d_q being independent of q (i.e., monofractal structure) would indicate a second-order phase transition in the system. On the other hand, if a final state is formed as a result of the self-similar cascade mechanism, one expects d_q to increase with q [4,8,9]. If we assume that the above considerations can be extrapolated to the processes of nuclear fragmentation, then one can expect that the study of the dependence of anomalous dimensions, measured for the fragment charge distributions, on the rank of the moments may allow one to distinguish between sequential (cascade like) and prompt (single fractal object) mechanisms. Furthermore if the system exhibits a monofractal structure, it would indicate the possible occurence of critical phenomena.

IV. INTERMITTENCY IN CHARGE DISTRIBUTION OF ALL PARTICLES

Following the previous analyses of the factorial moments for charge distributions of fragments [15,16], we study the charge spectrum of all fragments irrespective of their charges. Specifically, $Z_{\min}$ is set to 1, and all the singly charged particles released from the projectile, N_p, whether they are spectators or participants, are included in this analysis.

Figures 3(a) and 3(b) show log-log plots of the dependence of the factorial moments calculated according to Eq. (3) on the number of subdivisions, M of the whole $\Delta Z = 78$ interval for the full data sets available at 10.6 and <1 GeV/nucleon. The moments of ranks $q = 2-5$ are shown for which statistically significant results can be obtained.

Factorial moments of the same order and calculated for various bin sizes are strongly correlated because their computation is based on the successive rebinning of the same data. As a consequence the errors of the average factorial moments, estimated from the dispersion, D, of the values of the moments used to calculate the average, are overestimated (the variations between the points are much smaller than expected from the errors of the mean moments). In this analysis we have made an attempt to reduce the errors of correlated data points. The correlations between measured moments are due to event-to-event fluctuations of the total multiplicity and to bin-to-bin correlations. The fluctuations of the total multiplicity are reflected in the absolute values of the moments and in the dispersion of the moments calculated for $M = 1$, $D_{M=1}$. They also give a constant, independent of M, contribution to the errors of the moments calculated for $M > 1$. The bin-to-bin correlations are due to the overlap of bins corresponding to different M's, i.e., usually smaller bins are contained in larger ones. They give contribution to the errors, clearly dependent on M, which are important for studying the dependence of the moments on the width of the bin. Assuming that these two contributions are independent we have calculated, at each bin width, the dispersion D_{var}: $D^2_{\text{var}} = D^2 - D^2_{M=1}$. The errors of the mean moments calculated from the dispersion D_{var} are shown in the figures and included in the fits.

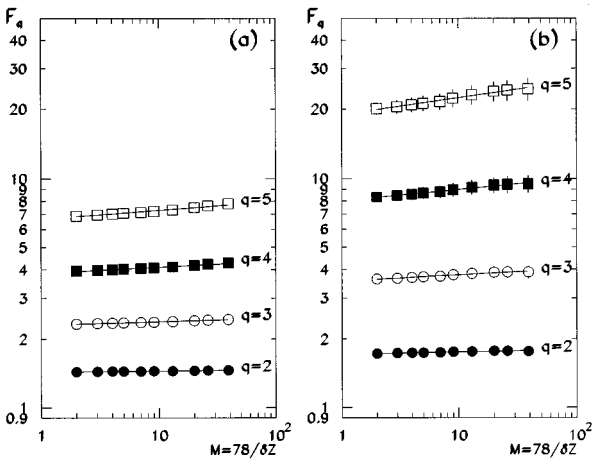

FIG. 3. log-log plots of the factorial moments F_q calculated with $Z_{\min} = 1$ for full data sets at 10.6 GeV/nucleon (a) and at 0.1–1 GeV/nucleon (b). Full circles correspond to $q = 2$, open circles to $q = 3$, full squares to $q = 4$, and open squares to $q = 5$. Lines show the best fits to power law functions.

A clear intermittency signal is seen (Fig. 3) at both energies indicated by a power law increase of the moments with decreasing δZ. At lower energy the rise of the moments is faster suggesting a stronger intermittency effect in <1 GeV/nucleon data than at 10.6 GeV/nucleon.

In [15] the analysis of the factorial moments was done for

TABLE II. Average fragment multiplicities measured in selected samples of events at 10.6 GeV/nucleon and 0.1–1 GeV/nucleon.

Sample	^{197}Au (10.6 GeV/nucleon)		^{197}Au (0.1–1 GeV/nucleon)	
	$N_F \geq 3$	$N_{\text{fr}} = 29-55$	$N_F \geq 3$	$N_{\text{fr}} = 29-55$
N_{events}	320	332	137	93
$\langle N_p \rangle$	32.79 ± 0.73	32.95 ± 0.42	23.96 ± 1.11	27.12 ± 0.73
$\langle N_\alpha \rangle$	5.99 ± 0.15	6.36 ± 0.14	7.37 ± 0.27	8.55 ± 0.28
$\langle N_F \rangle$	3.69 ± 0.05	3.07 ± 0.08	3.92 ± 0.10	3.75 ± 0.15

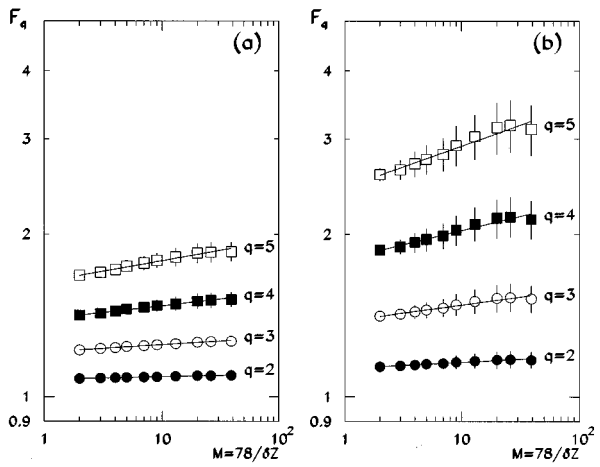

FIG. 4. The same as in Fig. 3 but for events with the number of heavy fragments $N_F \geq 3$ for 10.6 GeV/nucleon (a) and 0.1–1 GeV/nucleon (b).

selected subsamples of events in order to search for a class of events which exhibits the strongest intermittency signal. Two different selection criteria were applied: one limiting the analysis to multifragmentation events for which the number of heavier fragments, N_F, exceeds some threshold value and one restricting the total multiplicity of fragments. Similar selection criteria were applied to our data samples. Specifically, (a) $N_F \geq 3$, and (b) $N_{\rm fr}=N_p+N_\alpha+N_F=29{:}55$. In Table II the event statistics and average multiplicities of different fragments are listed for subsamples selected according to each of the above criteria at 10.6 GeV/nucleon and 0.1–1 GeV/nucleon. Plots of the factorial moments are shown in Figs. 4(a), 4(b), and 5(a) and 5(b) for these two classes of events. For each set of events the moments follow a linear rise with M in log-log plots, although this rise is strongly suppressed for the events with restricted $N_{\rm fr}$ multiplicity [Fig. 5, criterion (b)].

The power law fits to the dependencies shown in Figs. 3–5 were performed for $39 \geq \delta Z \geq 2$. To account for the correlations between the moments calculated for different δZ

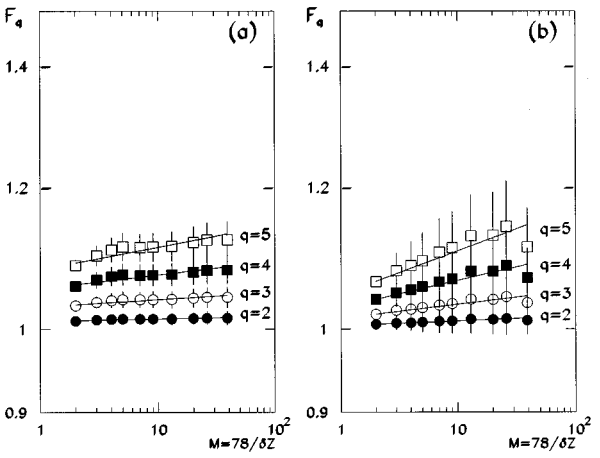

FIG. 5. The same as in Fig. 4 but for events with the total number of fragments $N_{\rm fr}=29{:}55$ for 10.6 GeV/nucleon (a) and 0.1–1 GeV/nucleon (b).

TABLE III. Intermittency indices φ_q from power law fits to the factorial moments calculated with $Z_{\rm min}=1$ for different event selections. The upper values are for 10.6 GeV/nucleon data, the lower values are for 0.1–1 GeV/nucleon data.

Sample	All events	$N_F \geq 3$	$N_{\rm fr}=29{:}55$
φ_2	0.005 ± 0.004	0.005 ± 0.003	0.001 ± 0.002
	0.010 ± 0.011	0.011 ± 0.008	0.003 ± 0.004
φ_3	0.015 ± 0.005	0.014 ± 0.005	0.004 ± 0.003
	0.027 ± 0.017	0.030 ± 0.012	0.008 ± 0.006
φ_4	0.026 ± 0.007	0.026 ± 0.007	0.008 ± 0.004
	0.049 ± 0.023	0.053 ± 0.018	0.015 ± 0.008
φ_5	0.039 ± 0.009	0.039 ± 0.009	0.013 ± 0.005
	0.073 ± 0.030	0.078 ± 0.023	0.024 ± 0.010

one should perform fully correlated fits including the whole covariance matrix [34]. However, for low statistics data the determination of the covariance matrix is not sufficiently accurate to assure the reliable results of the fit. Therefore, in the present analysis the standard uncorrelated fits were done. We have checked, however, that the fits containing the full covariance matrix, determined from our presently available data, gave similar values of the intermittency indices but with frequently smaller errors as compared to those obtained from uncorrelated fits and reported in this paper.

The values of the fitted intermittency indices, φ_q, for dif-

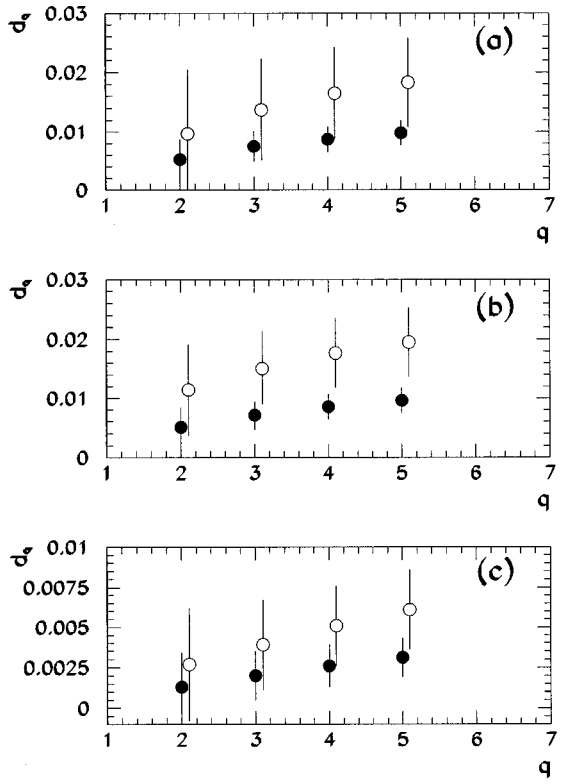

FIG. 6. Dependencies of the anomalous dimensions d_q on the order of the moments for 10.6 GeV/nucleon data (full circles) and 0.1-1 GeV/nucleon data (open circles) for different event selections: all events (a); events with $N_F \geq 3$ (b); and events with $N_{\rm fr}=29-55$ (c).

TABLE IV. Intermittency indices φ_q from power law fits to the factorial moments calculated with $Z_{\min}=1$, but for different selections of singly charged particles, for the two 10.6 GeV/nucleon data samples.

Sample	$\theta_{\rm cut}$	$\langle N_p(\theta\leqslant\theta_{\rm cut})\rangle$	φ_2	φ_3	φ_4	φ_5
All	0.011	5.06±0.10	−0.006±0.004	−0.011±0.007	−0.013±0.011	−0.009±0.016
events	0.023	11.54±0.22	−0.001±0.004	0.001±0.006	0.005±0.009	0.015±0.014
	0.034	16.46±0.33	0.001±0.003	0.006±0.005	0.014±0.008	0.024±0.011
	0.048	20.96±0.44	0.003±0.003	0.010±0.005	0.020±0.007	0.031±0.010
$N_F\geqslant 3$	0.011	6.24±0.16	0.006±0.005	0.018±0.007	0.032±0.010	0.047±0.014
	0.023	14.51±0.30	0.005±0.004	0.016±0.006	0.030±0.008	0.046±0.011
	0.034	20.07±0.41	0.005±0.004	0.015±0.005	0.027±0.008	0.042±0.010
	0.048	24.83±0.54	0.005±0.004	0.015±0.005	0.028±0.007	0.043±0.010

ferent data sets at low and high energies are listed in Table III. For the full data sets and also for events with $N_F\geqslant 3$, we observe systematically a stronger intermittency effect at lower energy. Selection of events with multiple emission of heavier fragments gives a stronger intermittency signal with respect to the selection on $N_{\rm fr}$ multiplicity.

Figure 6 shows the anomalous dimensions d_q calculated from Eq. (5) as a function of the rank of the moments. That d_q increases with q suggests that the fragmentation of gold projectiles proceeds via a sequential or cascadelike mechanism.

In the analyses presented above all singly charged particles (N_p) were included, although only a fraction of these particles ($N_{\rm spect}$) are associated with the process of gold fragmentation. Since the number of these singly charged particles is much larger than the number of multiply charged fragments (see Table I) they exert a significant and uncertain influence on the results. We made an attempt to distinguish between the spectator singly charged particles and participant protons on an event by event basis using the measured emission angles of the singly charged particles released from the projectile. It can be assumed that spectators are emitted at smaller angles than participants, which have suffered an energy loss and acquired some transverse momentum, due to the interactions with target nucleons. Therefore, by selecting only those of the N_p particles which are emitted in the laboratory system within a very narrow forward angle, $\theta\leqslant\theta_{\rm cut}$, we are enriching our sample of analyzed particles by singly charged spectators. Such a procedure could be applied to our 10.6 GeV/nucleon data where the emission angles of all charged particles originated from the interaction vertex have been precisely measured. The results are quoted in Table IV which lists the values of the fitted intermittency exponents obtained from the analysis comprising only those singly charged particles from a given event which fulfill the criterion $\theta\leqslant\theta_{\rm cut}$. The analysis was performed for the full data sample as well as for a subsample of events with $N_F\geqslant 3$. The $\theta_{\rm cut}$ values varied from 0.011 rad up to 0.048 rad. The corresponding average multiplicities of singly charged particles fulfilling a given angular criterion are also listed in Table IV.[2] Inspecting the φ_q values given in Table IV and comparing them to those listed in Table III (corresponding to the inclusion of all N_p particles) we see a distinct difference in the dependence of the slopes on the number of the analyzed singly charged particles between the full data set and the set of events with $N_F\geqslant 3$. While for the full sample we observe a strong decrease of the intermittency indices with decreasing multiplicity of singly charged particles, for events with at least three heavy fragments the indices weakly depend on the $\langle N_p(\theta\leqslant\theta_{\rm cut})\rangle$. Nevertheless, although we were not able to unambigously identify the spectators, the applied approximate procedure has shown that for all events without any selection, the intermittency effects are due to the singly charged particles, and restricting the number of these particles ultimately leads to the disappearance of the intermittency fluctuations, i.e., indices $\varphi_q<0$ (this will be also seen from the analysis which follows).

V. FACTORIAL MOMENTS OF CHARGE DISTRIBUTIONS OF MULTIPLY CHARGED FRAGMENTS

To avoid the uncertainties due to the unknown number of singly charged spectators in a given event, it is reasonable to restrict the intermittency analysis to only multiply charged fragments ($Z\geqslant 2$). Thus we now set $Z_{\min}=2$ and repeat the analysis.

Figures 7(a) and 7(b) show the factorial moments as a function of M for the full datasets, and the moments are not compatible with a power law. The observed convexity in the behavior of the moments indicates that intermittency patterns are not present in the Z distributions of multiply charged fragments. This agrees with the trend we have seen from the above study of the dependence of the intermittency on the number of singly charged particles accepted for the analysis.

On the other hand for the subsample of multifragmentation events corresponding to $N_F\geqslant 3$ the moments increase like a power function with decreasing width of the charge bins in the range $\delta Z\geqslant 2$, as is shown in Figs. 8(a) and (b). The fitted intermittency exponents are given in Table V. Comparing the values quoted in Table V with those listed in Table III shows that restriction of the analysis to multiply charged fragments reveals an enhanced signal of dynamical fluctuations in the fragment charge distributions for selected multifragmentation events as compared to the analysis presented in Sec. IV. This may indicate that the fluctuations

[2]It is worth noting that, for the full data set, the $\langle N_p(\theta\leqslant 0.048\ {\rm rad}\rangle$ coincides with the value which can be evaluated from the VENUS [35] model calculations. This model predicts that for Au-emulsion interactions the $\langle N_{\rm part}\rangle=9.4$ which corresponds to about 20 spectators ($\langle N_{\rm spect}\rangle=\langle N_p\rangle-\langle N_{\rm part}\rangle$).

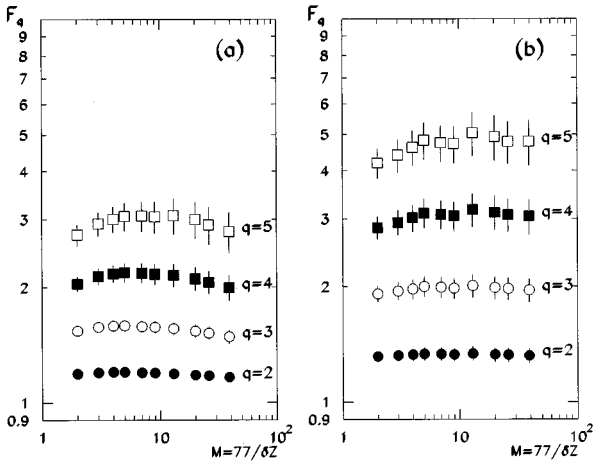

FIG. 7. log-log plots of the factorial moments F_q calculated with $Z_{\min}=2$ vs M for full data sets at 10.6 GeV/nucleon (a) and 0.1–1 GeV/nucleon (b). Different symbols correspond to different ranks of the moments (see caption to Fig. 3 for details).

among the multiply charged fragments are stronger. On the other hand, this observation can be also explained by the fact that the analysis of multiply charged fragments involves particles originating from a single source (fragmentation of gold nuclei) whereas in the previous analysis the particles from two distinct sources, namely from the fragmentation process (spectator protons and multiply charged fragments) and from the collision process (participant protons), are mixed.

In Figs. 9(a) (10.6 GeV/nucleon) and (b) (0.1–1 GeV/nucleon) we present the comparison of the φ_q values obtained for $Z_{\min}=1$ and $Z_{\min}=2$ for different subsamples of events selected according to cuts on N_F multiplicity. For all the selected subsamples, setting $Z_{\min}$ to 2 gives larger φ_q values than $Z_{\min}=1$ for 10.6 GeV/nucleon data. For the lower energy data, the evidence is not clear due to the larger errors, but the trend is, systematically $\varphi_q(Z_{\min}=2) > \varphi_q(Z_{\min}=1)$. The intermittency indices resulting from the analysis of multiply charged fragments show no significant energy dependence although systematically the values of the indices obtained for 10.6 GeV/nucleon data are smaller than those obtained for lower energy data.

Although the analysis of the gold fragmentation, based on a relatively low statistics emulsion data, revealed some interesting observations, it is evident that higher statistics are needed to confirm the above observations. It certainly would be interesting to perform such an analysis for high statistics electronic datasets [36,37].

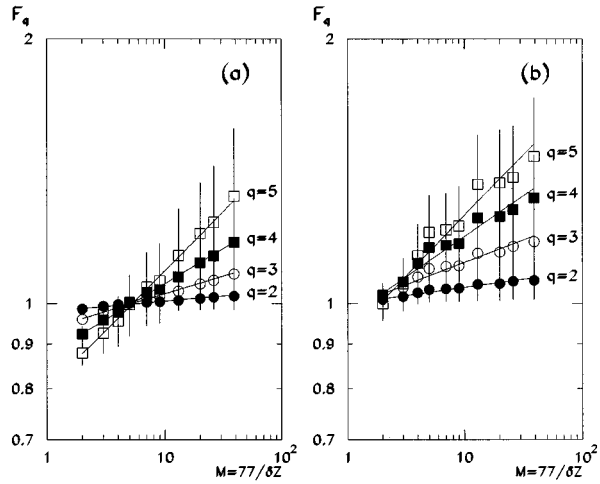

FIG. 8. The same as in Fig. 7 but for events with the number of heavy fragments $N_F \geq 3$ for 10.6 GeV/nucleon (a) and 0.1–1 GeV/nucleon (b). Lines show the fitted power law functions. Symbols are the same as in Fig. 3.

VI. SUMMARY AND CONCLUSIONS

The method of factorial moments was used to search for dynamical fluctuations in the charge distributions of frag-

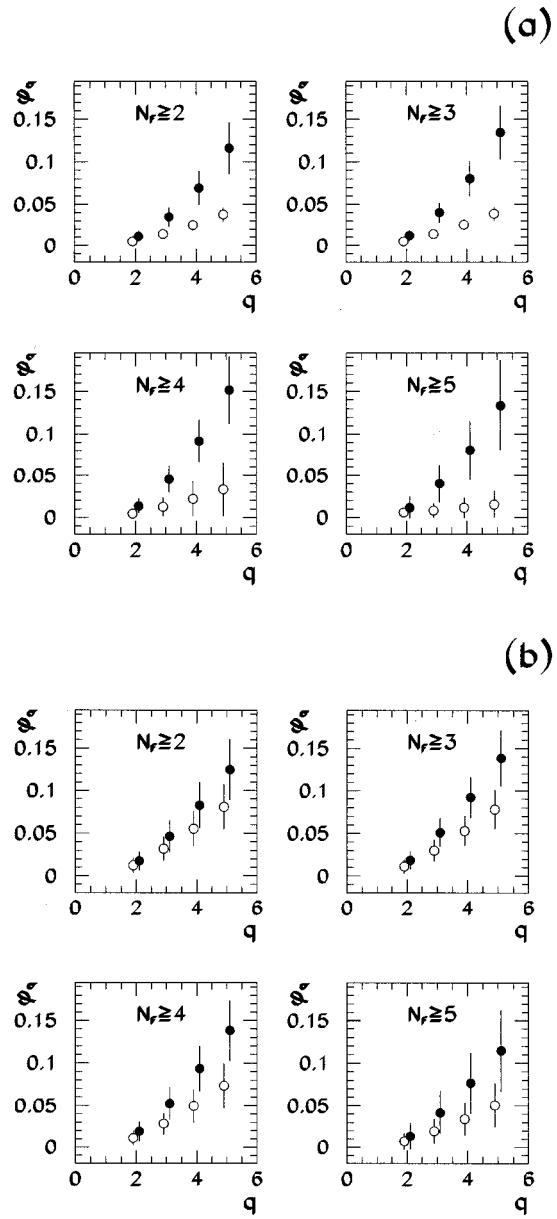

FIG. 9. Comparison of the intermittency indices obtained from fits to the factorial moments calculated with $Z_{\min}=1$ (open circles) and $Z_{\min}=2$ (full circles) for subsamples of events with different N_F multiplicities at 10.6 GeV/nucleon (a) and at 0.1–1 GeV/nucleon (b). Values of q are slightly displaced for clarity.

TABLE V. Intermittency indices φ_q from power law fits to the factorial moments calculated with $Z_{\min}=2$ for events with $N_F \geqslant 3$ at 10.6 GeV/nucleon and 0.1–1 GeV/nucleon.

	10.6 GeV/nucleon	0.1–1 GeV/nucleon
φ_2	0.012 ± 0.007	0.019 ± 0.011
φ_3	0.040 ± 0.012	0.051 ± 0.017
φ_4	0.080 ± 0.020	0.092 ± 0.025
φ_5	0.135 ± 0.032	0.139 ± 0.033

ments arising from deexcitation of gold projectiles after an interaction with emulsion nuclei at incident energy of 10.6 GeV/nucleon. For comparison, the same analysis was performed for gold fragmentation at energies $<$ 1 GeV/nucleon. The factorial moments were found to increase like a power law with decreasing width of the charge bin in the analysis of all particles ($Z=1-79$) released from the fragmenting gold projectiles. This evidence for the existence of nonstatistical fluctuations of the intermittent type confirms the previously reported results. Comparison of the results obtained for different projectile energies indicate that dynamical fluctuations are stronger at low energy than at 10.6 GeV/nucleon. It was also found that multifragmentation events exhibit stronger intermittency than the events with restricted fragment multiplicities.

It was shown that the results obtained for all minimum bias events are sensitive to the number of singly charged particles subjected to the analysis. The analysis, limited to multiply charged fragments only, revealed no intermittency when all events are used without any selection on the fragment multiplicity. On the other hand, some evidence for the intermittency effect was found for multifragmentation events. These multifragmentation events exhibit a stronger intermittency signal when compared to an analysis that also included the singly charged particles released from the gold projectiles. In the latter case, the mixing of particles originating from the two different processes may be responsible for the weaker fluctuations.

From the fitted intermittency indices, the anomalous fractal dimensions have been calculated and found to depend upon the order of the moments, in contradiction to the expectations from a prompt decay mechanism or a second-order phase transition. This dependence suggests the occurence of sequential decay in the fragmentation of gold nuclei.

The results, presented here on the observation of dynamical fluctuations in the charge distributions of fragments emanating from excited gold projectiles constitute a challenge for theory and/or models of nuclear multifragmentation. The problems which certainly need to be solved, within the framework of fragmentation models, are whether and how the charge conservation effects, which produce the holes in the fragment charge distributions, and the finite size of the decaying system affect the factorial moments and the strength of the intermittency signal. It is worth pointing out that for the multifragmentation events as well as the analysis of only multiply charged fragments, which both showed clear intermittency signals, charge conservation effects may be more substantial than in the case of the analysis of all events without any selection or the inclusion of singly charged particles.

ACKNOWLEDGMENTS

This work has been supported in Poland by the Committee for Scientific Research Grant No. 2P03B18409 and in USA at Louisiana State University by NSF Grant Nos. PHY-9213621 and INT-8913051 and at University of Minnesota by DOE Grant No. DOE-FG02-89ER40528.

[1] B. Mandelbrot, J. Fluid Mech. **62**, 331 (1974); U. Frisch, P. Sulem, and M. Nelkin, *ibid.* **87**, 719 (1978).
[2] Ya.B. Zeldovich *et al.*, Sov. Phys. Usp. **30**, 353 (1987).
[3] G. Paladin and A. Vulpiani, Phys. Rep. C **156**, 147 (1987).
[4] A. Białas and R. Peschanski, Nucl. Phys. **B273**, 703 (1986); **B308**, 857 (1988).
[5] For recent review see E.A. De Wolf *et al.*, University of Nijmegen Report No. HEN-362, 1993 [Phys. Rep. (to be published)].
[6] R. Hołyński *et al.*, Phys. Rev. Lett. **62**, 733 (1989); Phys. Rev. C **40**, R2449 (1989).
[7] J. Bachler *et al.*, Z. Phys. C **61**, 551 (1994).
[8] A. Białas and R. Peschanski, Phys. Lett. B **207**, 59 (1988).
[9] A. Białas and R.C. Hwa, Phys. Lett. B **253**, 436 (1991).
[10] Ph. Brax and R. Peshanski, Phys. Lett. B **253**, 225 (1991).
[11] W. Ochs, Z. Phys. C **50**, 339 (1991).
[12] N.G. Antoniou *et al.*, Phys. Lett. B **245**, 619 (1990); **293**, 187 (1992); Phys. Rev. D **45**, 4034 (1992).
[13] H. Satz, Nucl. Phys. **B326**, 613 (1989).
[14] R.C. Hwa and M.T. Nazirov, Phys. Rev. Lett. **69**, 741 (1992).
[15] M. Płoszajczak and A. Tucholski, Phys. Rev. Lett. **65**, 1539 (1990); Nucl. Phys. **A523**, 651 (1991).
[16] P.L. Jain *et al.*, Phys. Rev. Lett. **68**, 1656 (1992); G. Singh *et al.*, Mod. Phys. Lett. A **7**, 1113 (1992).
[17] J. Aichelin, Phys. Rep. **202**, 233 (1991).
[18] D. Stauffer, Phys. Rep. **54**, 1 (1979).
[19] B. Elattari, J. Richter, and P. Wagner, Phys. Rev. Lett. **69**, 45 (1992).
[20] C.J. Waddington and P.S. Freier, Phys. Rev. C **31**, 888 (1985).
[21] C.J. Waddington, Int. J. Mod. Phys. E **2**, 739 (1993).
[22] R. Hołyński, Nucl. Phys. **A566**, 191c (1994).
[23] M.L. Cherry *et al.*, Z. Phys. C **62**, 25 (1994).
[24] M.L. Cherry *et al.*, Z. Phys. C **63**, 549 (1994).
[25] B.S. Nilsen *et al.*, Phys. Rev. C **50**, 1065 (1994).
[26] L.G. Moretto and G.J. Wozniak, Annu. Rev. Nucl. Part. Sci. **43**, 379 (1993).
[27] W. Trautmann *et al.*, Z. Phys. A **344**, 447 (1993).
[28] L.Y. Geer *et al.*, Phys. Rev. C **52**, 334 (1995).
[29] M.L. Cherry *et al.*, Phys. Rev. C **52**, 2652 (1995).
[30] K. Fiałkowski, B. Wosiek, and J. Wosiek, Acta Phys. Pol. B **20**, 639 (1989).
[31] P. Lipa and B. Buschbeck, Phys. Lett. B **223**, 465 (1989).

[32] R.C. Hwa, Phys. Rev. D **41**, 1456 (1990).
[33] A.R. DeAngelis, D.H.E. Gross, and R. Heck, Nucl. Phys. **A537**, 606 (1992).
[34] B. Wosiek, Acta Phys. Pol. B **21**, 1021 (1990).
[35] K. Werner, Phys. Rev. D **39**, 780 (1989); CERN Report No. CERN-TH 5682, 1990.
[36] C.A. Ogilvie *et al.*, Nucl. Phys. **A553**, 271c (1993).
[37] J. Dreute *et al.*, Phys. Rev. C **44**, 1057 (1991).